Heterochrony and Early Left-Right Asymmetry in the Development of the Cardiorespiratory System of Snakes

Soldt, B.J. van; Metscher, B.D.; Poelmann, R.E.; Vervust, B.L.C.; Vonk, F.J.; Mueller, G.B.; Richardson, M.K.

Heterochrony and Early Left-Right Asymmetry in the Development of the Cardiorespiratory System of Snakes

Benjamin J. van Soldt[1], Brian D. Metscher[2], Robert E. Poelmann[3], Bart Vervust[4], Freek J. Vonk[1,5], Gerd B. Müller[2], Michael K. Richardson[1]*

1. Institute of Biology, University of Leiden, Leiden, the Netherlands, **2.** Department of Theoretical Biology, University of Vienna, Vienna, Austria, **3.** Department of Anatomy and Embryology, Leiden University Medical Center, Leiden, the Netherlands, **4.** Department of Biology, University of Antwerp, Antwerp, Belgium, **5.** NCB Naturalis, Leiden, the Netherlands

*m.k.richardson@biology.leidenuniv.nl

Abstract

Snake lungs show a remarkable diversity of organ asymmetries. The right lung is always fully developed, while the left lung is either absent, vestigial, or well-developed (but smaller than the right). A 'tracheal lung' is present in some taxa. These asymmetries are reflected in the pulmonary arteries. Lung asymmetry is known to appear at early stages of development in *Thamnophis radix* and *Natrix natrix*. Unfortunately, there is no developmental data on snakes with a well-developed or absent left lung. We examine the adult and developmental morphology of the lung and pulmonary arteries in the snakes *Python curtus breitensteini*, *Pantherophis guttata guttata*, *Elaphe obsoleta spiloides*, *Calloselasma rhodostoma* and *Causus rhombeatus* using gross dissection, MicroCT scanning and 3D reconstruction. We find that the right and tracheal lung develop similarly in these species. By contrast, the left lung either: (1) fails to develop; (2) elongates more slowly and aborts early without (2a) or with (2b) subsequent development of faveoli; (3) or develops normally. A right pulmonary artery always develops, but the left develops only if the left lung develops. No pulmonary artery develops in relation to the tracheal lung. We conclude that heterochrony in lung bud development contributes to lung asymmetry in several snake taxa. Secondly, the development of the pulmonary arteries is asymmetric at early stages, possibly because the splanchnic plexus fails to develop when the left lung is reduced. Finally, some changes in the topography of the pulmonary arteries are consequent on ontogenetic displacement of the heart down the body. Our findings show that the left-right asymmetry in the cardiorespiratory system of snakes is expressed early in development and may become phenotypically expressed through heterochronic shifts in growth, and changes in axial relations of

organs and vessels. We propose a step-wise model for reduction of the left lung during snake evolution.

Introduction

Pulmonary left-right asymmetry is an intriguing deviation from what is otherwise a mostly bilaterally symmetric body plan in vertebrates. To date, studies have focused on the developmental mechanisms of pulmonary asymmetry in mouse [1–3]. These studies show critical roles for Pitx2 [4], Tbx4 and Tbx5 [5]. In addition, studies in *Drosophila*, mouse and birds suggest that mechanisms of pulmonary development are highly conserved throughout the animal kingdom [6,7]. For example, *Drosophila branchless* and *breathless* are homologues to mammalian Fgf10 and Fgfr2b, respectively [8,9]. It thus seems likely that developmental mechanisms governing pulmonary left-right asymmetry in other species are similar to those in the mouse, so that current data may be used to study developmental mechanisms in other species.

Developmental mechanisms of pulmonary left-right asymmetry are not well understood in species groups outside mammals, although this is where many striking instances of this anatomical feature are found. One example is the snake respiratory system (see for reviews Refs. [10–14]). Briefly, the right lung in snakes is typically well-developed, while the left lung exhibits a range of anatomies that can be subdivided into an absent (type one), a vestigial (type two) and a well-developed type (type three) [12] (Table 1). The pattern of the pulmonary arteries varies in ways similar to the lungs (Table 1).

The various types of snake lung anatomies suggest distinct genetic alterations of the ancestral mechanism of pulmonary development. By investigating the development of these lung anatomies and comparing them to relevant outgroups, we may get a better understanding of the evolution of the snake respiratory system. A key question herein is which snake lung anatomy type represents the primitive condition. Previous work has designated the well-developed left lung (type three) as such [10]. Another study presents the vestigial left lung as being the primitive condition [12]. Currently there is no consensus on the verity of either of these hypotheses.

Schmalhausen [15] found that in the European grass snake *Natrix natrix* Linnaeus, 1758 (family Colubridae) (well-developed right lung and vestigial left lung [12]) the early lung bud is an evagination from the floor of the endodermal foregut, which then bifurcates into two bronchial buds (Fig. 1A). This early pattern is similar to that described in the mouse and human [3,16,17]). However, Schmalhausen stated that the right bronchial bud elongates more rapidly than the left one does (Fig. 1B, C) and continues growing at a later developmental stage than the left, whose growth ends prematurely. This 'truncation' of development is one kind of heterochrony (change in developmental sequence during evolution;

Table 1. Overview of some variations in the morphology of the lungs in selected snake taxa based on the literature.

|	Left lung					Right lung			Tracheal lung	
Character	Adult anatomy			Length of vascular portion of left lung	Length of saccular portion of left lung	Adult anatomy	Length of vascular portion of left lung	Length of saccular portion of left lung	Adult anatomy	
States [10, 12, 14, 75]	Absent	Vestigial	Well-developed	Varies widely depending on species	Varies widely depending on species	Well-developed	Varies widely depending on species	Varies widely depending on species	Present	Absent
State of associated pulmonary artery [54–56, 60, 71, 76–82]	Absent left pulmonary artery	Absent or reduced left pulmonary artery	Present left pulmonary artery	Depending on species, left pulmonary artery extends throughout the entire vascular lung, or is overtaken by right pulmonary artery.	No left pulmonary artery associated with saccular left lung	Present right pulmonary artery	Right pulmonary artery extends throughout all of the vascular lung	No right pulmonary artery associated with saccular right lung	Present anterior pulmonary artery	Absent anterior pulmonary artery
Representative taxa	Acrochordidae	Colubridae	Boidae			All examined snakes			Acrochordidae	Boidae

reviewed in Refs. [18–23]). Similar findings were found in the Plains garter snake *Thamnophis radix* Baird and Girard, 1853 (family Colubridae) [24], which has an adult pulmonary anatomy similar to that of *Natrix natrix* (see also Ref. [12] for a review). While these studies suggest that pulmonary asymmetry is determined during early stages of lung development by heterochrony, without developmental data on snake species with a well-developed or absent left lung in the adult, the issue remains unresolved.

Regarding pulmonary artery development, studies in chick, mouse and man [2, 25–31] show that the pulmonary arteries develop from splanchnic plexi, surrounding the developing lung buds [25, 30–32]. When the pulmonary trunk and the sixth pharyngeal arch artery (PAA) have formed, microvasculature from the lungs connects with this PAA pair, the two coming into vascular continuity. Stabilization by smooth muscle cells forms the definitive pulmonary artery [25, 31, 33]. With exception of establishment of the pulmonary trunk [34–39], little is known about these events in reptiles other than birds.

In this study, we first categorize the pulmonary artery and lung anatomies of adult snakes from a range of taxa. We then use these typifications to examine the development of the snake lung and pulmonary artery, using series of embryos of five species of snake: (i) Malayan pit viper *Calloselasma rhodostoma* Kuhl, 1824, family Viperidae; (ii) common night adder *Causus rhombeatus* Liechtenstein, 1823, family Viperidae; (iii) corn snake *Pantherophis guttata guttata* Linnaeus, 1766, family Colubridae; (vi) midland rat snake *Elaphe obsoleta spiloides* Duméril,
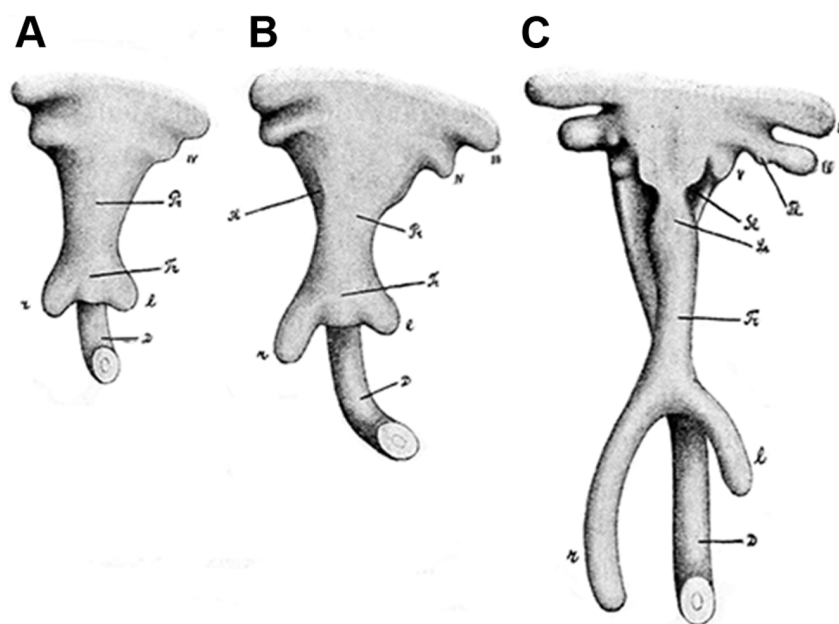
Fig. 1. Early lung development in *Natrix natrix* according to Schmalhausen. Overview figure showing three subsequent stages of lung development in the snake *Natrix natrix*, a snake reported [12] to have a vestigial left lung. d: esophagus; l = left lung bud; r = right lung bud; tr = trachea. Adapted from Figures 5–7 in Ref. [15].

doi:10.1371/journal.pone.0116416.g001

1854, family Colubridae; and (v) blood python *Python curtus breitensteini* Schlegel, 1872, family Pythonidae. Due to limited material availability, we use a 22 days-after-oviposition (dao) specimen of *Elaphe obsoleta spiloides* to complement the *Pantherophis guttata guttata* specimens, since these snake species have similar pulmonary anatomies [12]. The same applies to *Calloselasma rhodostoma* and *Causus rhombeatus*. However, *Causus rhombeatus* is known to have a thoraconuchal lung (continuous tracheal/right lung), while in *Calloselasma rhodostoma* tracheal and right lung are distinct [12].

Materials and Methods

Ethics Statement

Under the active Dutch legislation at the time the study was performed (2011–2012), experiments with snake embryos were not considered to be animal experiments while the embryo was not free feeding, i.e. pre-hatching (Art. 1, Experiments on Animals Act (Wet op de Dierproeven)). Ethical review and advice of the animal experiments committee was therefore not required for this study. Still, the Leiden University animal welfare officer was approached for advice and

approval. Dutch animal experimentation legislation is based on the Guidelines on the protection of experimental animals by the Council of Europe, Directive 86/609/EEC.

Adult (Table 2) and embryonic (Table 3) snakes were from the zoology collection of the Institute of Biology, University of Leiden. Adult snakes were donated to the Institute of Biology by Dutch or Belgian pet owners as carcasses after the animals had died from natural causes. Specimens were fixed and stored in 70% ethanol upon donation. Embryos of *Causus rhombeatus and Calloselasma rhodostoma* were donated to the Institute of Biology; the other species' embryos were purchased from Dutch pet owners. All embryos were acquired while still alive, incubated at 28°C in a Heraeus B5060E incubator (Hanau, Germany) and euthanized instantly at various stages by fixating them in 4% paraformaldehyde (PFA) overnight at 4°C. They were then dehydrated in methanol, staged according to Zehr [40] (cross-checked with other staging tables [41–45]) and stored in 100% methanol at −20°C. For ages of euthanization, see Table 3. Incubation times vary wildly between snake species and are largely dependent on incubation temperatures. In our hands, at temperatures between 25°C and 29°C: *Calloselasma rhodostoma* embryos hatch after 32 − 39 days, *Causus rhombeatus* after 75 − 80 days, *Elaphe obsoleta spiloides* after 50 − 76 days, *Pantherophis gutta guttata* after 53 − 62 days, and *Python curtus breitensteini* after 58 − 65 days (at 32°C).

Pulmonary artery typifications

Adult snakes were measured (snout to cloaca and cloaca to tail-tip) and subsequently opened using a ventral midline incision using standard dissection equipment. The mesenteries were removed to expose the viscera. The heart, lung or lungs, and great vessels were examined by gross dissection, both *in situ* and after removal from the animal. A phylogeny of all the species studied, based on Refs. [12, 46–50], is shown in Fig. 2. For lung and pulmonary artery typifications in adult snakes we gathered data from 28 published studies (S1 Table) and our own dissections.

MicroCT imaging and Amira segmentation

For x-ray contrast enhancement, embryos were stained for one to four days in 1% phosphotungstic acid (PTA) dissolved in 100% methanol [51, 52]. Samples were then brought back to clean 100% methanol and mounted for scanning in plastic tubes or large pipette tips [53]. Attenuation-based microtomographic images were made using an Xradia MicroXCT system (Carl Zeiss X-Ray Microscopy, Pleasanton, CA), with a tungsten source (Hamamatsu L9421-02) set at 40 kV and 100 mA (4W) for a nominal spot size of 5μm. Projection images were taken every 0.2° over a rotation of 180° plus the imaging cone angle (usually 2–6° – thus 921–961 images per scan). Images were acquired with pixel sizes of 4–10μm, and tomographic reconstructions were made with the resident software (XMReconstructor) using a beam-hardening correction of 0.4 and 2×2 binning,

Table 2. Snake specimens used here to study snake lungs and pulmonary artery anatomy and the associated results.

| Species	Number analyzed	Common name	Family	Subfamily	Tracheal lung	Right lung anatomy	Left lung anatomy	PA*
Acrochordus granulatus	2	Wart snake	Acrochordidae	N/A	Present	Full	Absent	PA1
Eunectes notaeus	1	Yellow ana-conda	Boidae	Boinae	Absent	Full	Full	PA3
Morelia viridis	2	Green tree python	Boidae	Pythoninae	Absent	Full	Full	PA3
Python regius	5	Ball python	Boidae	Pythoninae	Absent	Full	Full	PA3
Lampropeltis triangulum sinaloae	1	Scarlet king-snake	Colubridae	Colubrinae	?	Full	Vestigial	PA2
Pantherophis guttata guttata	7	Corn snake	Colubridae	Colubrinae	Present	Full	Vestigial	PA2
Bungarus candidus	1	Blue krait	Elapidae	Elapinae	Present	Full	Vestigial	PA2
Bungarus fasciatus	1	Banded krait	Elapidae	Elapinae	Yes	Full	Vestigial	PA2
Hydrophis elegans	3	Elegant sea-snake	Elapidae	Hydrophiinae	Yes	Full	Absent	PA1
Natrix tessellata	3	Dice snake	Natricidae	Natricinae	Yes	Full	Vestigial	PA2
Thamnophis sirtalis concinnus	1	Common gar-ter snake	Natricidae	Natricinae	Absent	Full	Vestigial	PA2
Calloselasma rhodostoma	3	Malayan pit viper	Viperidae	Crotalinae	Yes	Full	Vestigial	PA1
Trimeresurus sp.	1	Pit viper	Viperidae	Crotalinae	Yes	Full	Vestigial	PA1

*PA = Pulmonary artery.

Table 3. Snake embryo specimens used here to study the development of the snake pulmonary arteries and lungs.

Species	Age (dao*)	Zehr stage [40]	Jackson stage [41]	Khannoon stage [42]	Boughner/Buchtová stage [44, 45]	Lung anatomy type [12]	PA** type
Calloselasma rhodostoma	3.00	26	1	2	1	Type 1	PA1
Calloselasma rhodostoma	20.00	36/37	8	8	7/8	Type 1	PA1
Causus rhombeatus	5.00	25	1	1	1	Type 1	PA1
Causus rhombeatus	8.00	28	1/2	2	1/3	Type 1	PA1
Causus rhombeatus	10.00	30	3	3/4	3	Type 1	PA1
Elaphe obsoleta spiloides	22.00	34	8	6	6/7	Type 2	PA2
Pantherophis guttata guttata	2.00	25	1	1	1	Type 2	PA2
Pantherophis guttata guttata	6.00	26	2	2	1/3	Type 2	PA2
Pantherophis guttata guttata	9.00	27	3	3	3	Type 2	PA2
Pantherophis guttata guttata	12.00	33	5	5/6	4/6	Type 2	PA2
Python curtus breitensteini	2.00	24	1	1	1	Type 3	PA3
Python curtus breitensteini	5.00	28	2	2	1/3	Type 3	PA3
Python curtus breitensteini	10.00	30	3/4	3	3/4	Type 3	PA3
Python curtus breitensteini	14.00	32	5	4	4	Type 3	PA3

*dao = days after oviposition.
**PA = Pulmonary Artery.
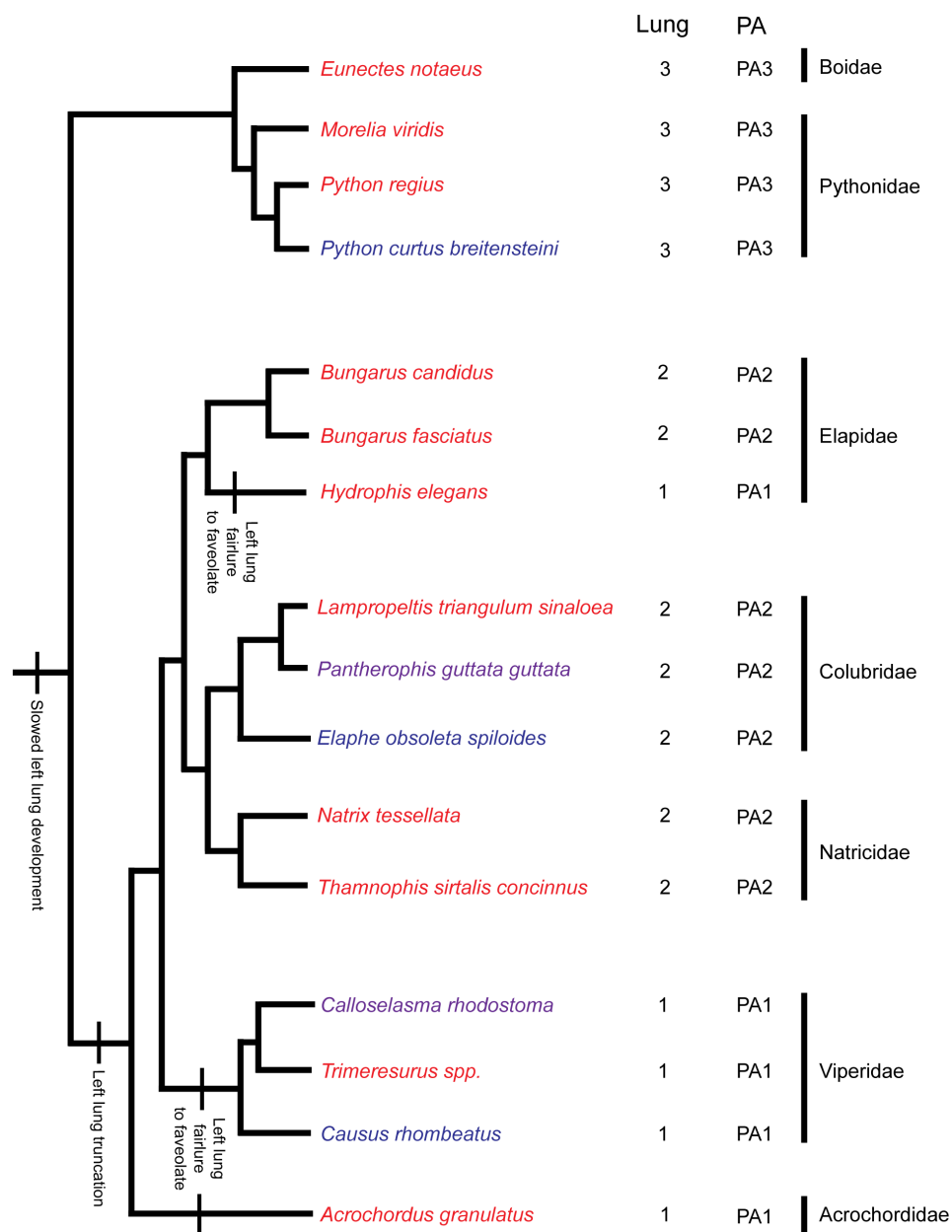
Fig. 2. Phylogeny of species used, with our hypothesis of the lung reduction steps mapped on. Red species were used for lung typification only, blue species for lung and vascular development only, and purple species for both. 'Lung' and 'PA' give lung type [12] and pulmonary artery type (Fig. 4), respectively. Stem and family branches are based on Refs. [46–48, 50]; the branches within families are based on Refs. [12, 49, 50].

doi:10.1371/journal.pone.0116416.g002

resulting in final voxel sizes of 8–20μm. Reconstructed images were exported as TIFF and loaded into Amira version 5.4 for annotation. We annotated the lumina of the blood vessels and lungs (Fig. 3; bright red outlines), but in the youngest stages we included epithelium (Fig. 3; astral blue, dark yellow and dark red outlines).
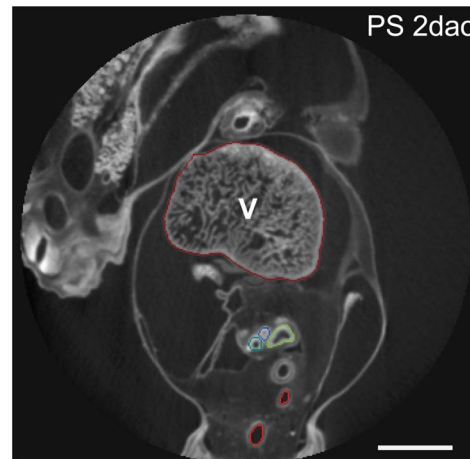
Fig. 3. Example of annotation methods in Amira 5.4.5. Dorsal side is up. V = ventricle. Scale bar represents 1 mm.

Results

Classification of the adult pulmonary arteries

Based on our dissections (Table 2) and the literature (S1 Table), all snakes have a single arterial pulmonary trunk arising from the ventricle. When it reaches roughly the top of the left atrium, the pulmonary artery may bifurcate, so that we can distinguish pulmonary artery anatomies based on two key characteristics of the vessels: (i) The number of pulmonary arteries: there may be one or two primary branches, and (ii) The direction in which the vessels run: they run either anteriorly or posteriorly.

Our classification is summarized in Table 4. Schematic illustrations showing these types can be seen in Fig. 4, and photographs showing typical examples of the types can be seen in Figs. 5–8. As we aimed for a generalized, gross typification, we only took the main branches into account. See Fig. 2 for a phylogeny that summarizes the results for the snakes dissected by us.

Embryonic development of the lungs and pulmonary arteries

Material used is listed in Table 3, and a legend to the color-coding of the Amira models is in Fig. 9. Figs. 10–12 show transverse sections just posterior to tracheal bifurcation or the tracheal lung of all specimens showing lung lumina. The Amira reconstructions can be viewed in Figs. 13–17. An overview of the developmental types described, cross-referenced with adult anatomies, is given in Table 5.

Zehr [40] stage 24–25

The extent of development of the heart and lungs varied considerably among our species sample at this stage. In *Pantherophis guttata guttata* (Fig. 13A), the tracheoesophageal septum had not formed, so that esophagus and trachea were

Table 4. Classification of observed pulmonary artery anatomies.

| Our classification	Pulmonary trunk	Taxonomic distribution in our samples	Figures
PA1	Trunk curves to the right, then bifurcates into anterior and posterior branches	Hydrophiinae, Acrochordidae and Crotalinae (*Acrochordus granulatus, Hydrophis elegans, Calloselasma rhodostoma, Trimeresurus sp.*)	5B, 6A,B
PA2	No bifurcation; continues as a single, descending pulmonary artery	Colubrinae, Natricinae and Elapinae (*Lampropeltis triangulum sinaloae, Pantherophis guttata guttata, Bungarus candidus, Bungarus fasciatus, Natrix tessellata*)	7A,B
PA3	Bifurcates into right and left branches descending on the dorsal side of the heart	Boinae and Pythoninae (*Eunectes notaeus, Morelia viridis, Python regius*)	8A,B

doi:10.1371/journal.pone.0116416.t004

still in continuity; this was not the case in the other species. In *P. guttata guttata* the right lung was longer than the left, but both had a distinct lumen distally (Fig. 10A). In *Python curtus breitensteini* (Fig. 13A) the right lung was longer than the left, but both featured a distinct lumen (Fig. 11A). In *Causus rhombeatus* (Fig. 12A; Fig. 13C) the left lung was absent.

P. guttata guttata (Fig. 13A) still had a common outflow tract. In *P. curtus breitensteini* (Fig. 13B) however, the outflow tract was divided into three channels: the left aorta, right aorta and the pulmonary channel. Finally, in *Causus rhombeatus* (Fig. 13C) only the aorticopulmonary septum had formed, dividing the outflow tract into a common aortic and a pulmonary channel. Regardless of developmental stage, the PAAs were in continuity with the two dorsal aortae, which originate from the ventricle. *P. curtus breitensteini* (Fig. 13B) was the only species to show two pulmonary arteries at this stage. Each artery extended to its respective lung from the sixth aortic arch; both ductus arteriosi were therefore distinct.

Zehr [40] stage 25–28
The esophagus and trachea in *P. guttata guttata* (Fig. 14A) were now separated by the trachea-esophageal septum. The right lung had elongated and acquired a distinct lumen in all species (Fig. 10B, Fig. 11B, Fig. 12B). The left lung in *P. curtus breitensteini* (Fig. 14B) was at a comparable stage of development to the right lung. By contrast, the left lung of *P. guttata guttata* (Fig. 14A) was smaller than the right and had only a small lumen distally, while the right also had distinct lumina at more anterior locations (Fig. 10B). In *Causus rhombeatus* (Fig. 14C) the tracheal lung could be identified for the first time as a thickening of the trachea at the level of the widening of the tracheal lumen. Posteriorly, the lumen widened more, denoting the start of the right lung (Fig. 12B; Fig. 14C).

With the establishment of the definitive left aorta, right aorta and pulmonary trunk, the vascular anatomy was now similar in all species. Except for *P. curtus breitensteini* (Fig. 14B), no pulmonary arteries had formed, although a layer of mesenchymal tissue (Fig. 10B) around the lungs in both *P. guttata guttata* and
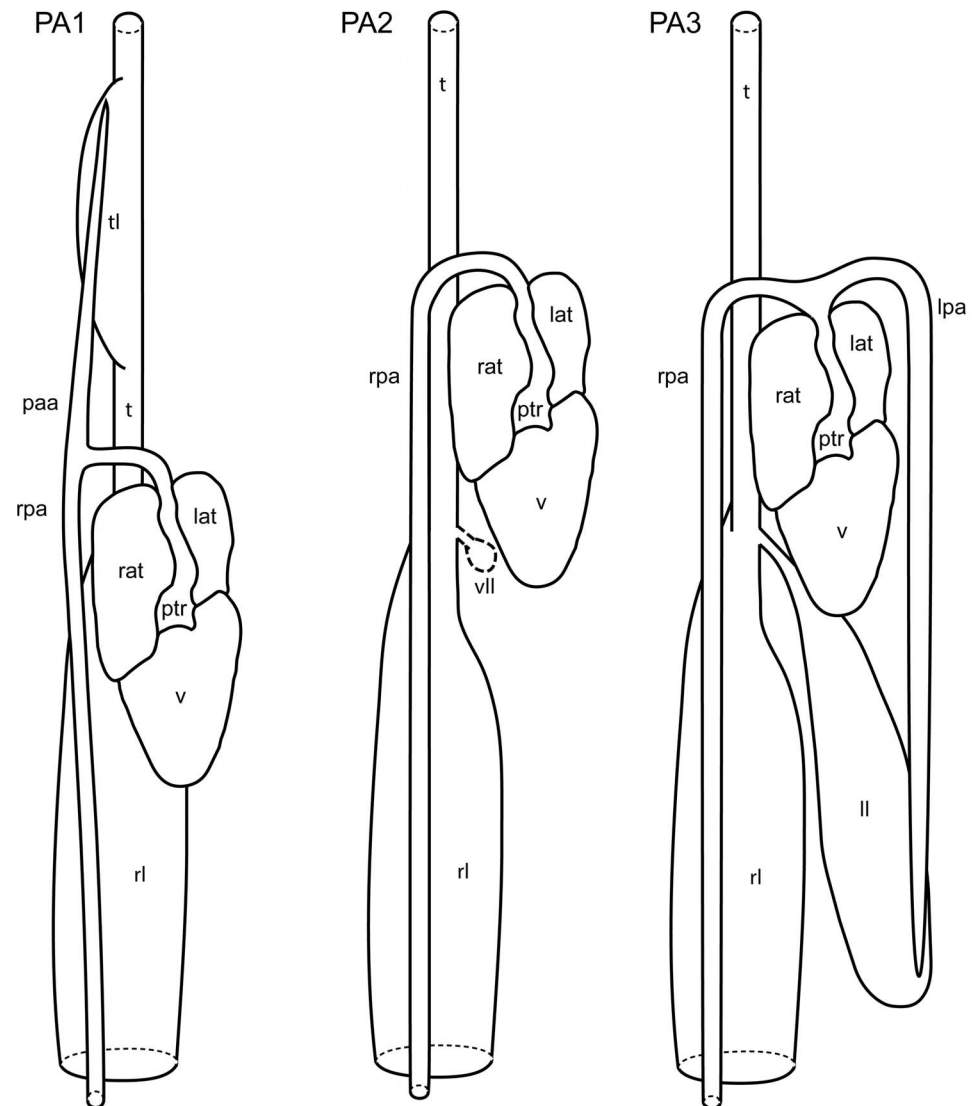
Fig. 4. Schematic portrayal of pulmonary artery types and the lungs to which they connect. Ventral views. PA1: pulmonary trunk that bifurcates into an ascending branch (connects with tracheal lung; tl) and a descending branch on the right (connects with the right lung; rl). PA2: single pulmonary artery, descending posteriorly and connecting to the right lung (rl); PA3: pulmonary trunk that bifurcates into two descending branches, each connecting to its respective lung (rl and ll); lat = left atrium; lpa = left pulmonary artery; pa = pulmonary artery; paa = anterior pulmonary artery; rat = right atrium; ptr = pulmonary trunk; rpa = right pulmonary artery; t = trachea; v = ventricle.

Causus rhombeatus might be interpreted as the splanchnic plexus from which the distal parts of the pulmonary arteries will develop.

Zehr [40] stage 26–30

The right lung had reached a similar stage of development in all species (Fig. 15A, B, C). In *P. guttata guttata* (Fig. 10C, Fig. 15A), no significant changes were observed. The left and right lungs in *P. curtus breitensteini* were equally developed
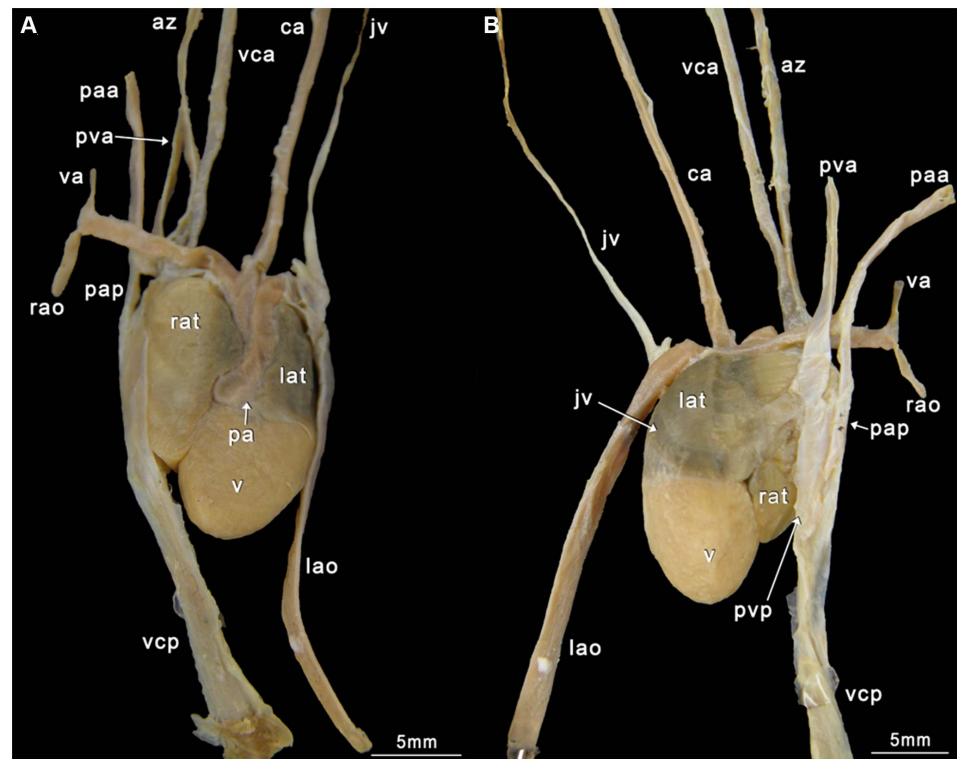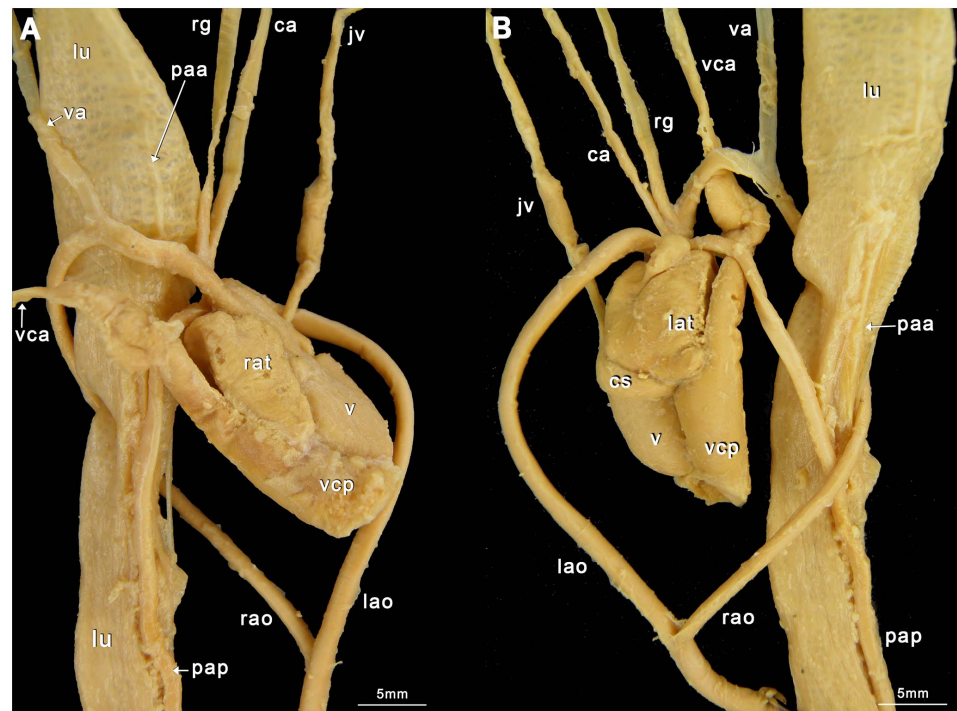
Fig. 5. The *Trimeresurus* spp. Heart (ID PK07). A Ventral view; B Dorsal view. az = azygos vein; ca = carotid artery; jv = jugular vein; lao = left aorta; lat = left atrium; lu = lung; paa = pulmonary artery anterior; pap = pulmonary artery posterior; pva = pulmonary vein anterior; pvp = pulmonary vein posterior; rao = right aorta; rat = right atrium; v = ventricle; va = vertebral artery; vca = vena cava anterior; vcp = vena cava posterior.

([Fig. 15B](#)). *Causus rhombeatus* and *Calloselasma rhodostoma* both had a tracheal lung (positioned anteriorly to the heart) and a right lung ([Fig. 15C, D](#)), but the right lung of *Calloselasma rhodostoma* was more obvious due to a constriction at cardiac level and luminal widening distally from this constriction ([Fig. 12D](#)); *Causus rhombeatus* lacked such a constriction and widening, a characteristic of a thoraconuchal lung ([Fig. 12C](#)).

At this stage, all species had one or two pulmonary arteries, arising posterior to the heart and connecting to their respective 6th PAA, although their point of origin could not be found. So, the pulmonary artery originating at the right lung connects to right 6th PAA. A left and right ductus arteriosus can be defined. At this developmental stage, the tracheal lung, where present, was not supplied by an obvious pulmonary artery; thus in both *Causus rhombeatus* ([Fig. 15C](#)) and *Calloselasma rhodostoma* ([Fig. 15D](#)) the pulmonary artery did not extend anterior to the heart. Possibly the tracheal lung was supplied with blood by a different vessel, or the anterior pulmonary artery was too small in diameter to be noticed or visualized reliably. If PFA did not bind with these thin vessels, it would not have appeared on the scans. Finally, *Causus rhombeatus* ([Fig. 15C](#)) had two pulmonary

Fig. 6. The *Hydrophis elegans* Heart (ID BS22). A Ventral view; B Dorsal view. ca = carotid artery; jv = jugular vein; lao = left aorta; lat = left atrium; lu = lung; paa = pulmonary artery anterior; pap = pulmonary artery posterior; pva = pulmonary vein anterior; pvp = pulmonary vein posterior; rao = right aorta; rat = right atrium; v = ventricle; va = vertebral artery; vca = vena cava anterior; vcp = vena cava posterior.

doi:10.1371/journal.pone.0116416.g006

arteries that both lead to the single, right lung. Finally, *Calloselasma rhodostoma* ([Fig. 15D](#)) featured two left 6th PAAs.

Zehr [40] stage 32–35

Specimens of *Calloselasma rhodostoma* or *Causus rhombeatus* were not available. Lung development in both *P. guttata guttata* ([Fig. 16A](#)) and *P. curtus breitensteini* ([Fig. 16B](#)) had reached a stage, at which separate faveoli became distinguishable. In *P. guttata guttata* ([Fig. 16A](#)) the left lung now featured a distinct lumen ([Fig. 10D](#)). Furthermore, the left lung was now in a more ventral location with respect to the right lung, compared with previous stages of this species examined.

Both *P. guttata guttata* ([Fig. 16A](#)) and *P. curtus breitensteini* ([Fig. 16B](#)) show changed spatial relations of the heart with respect to the PAAs: these are now located directly anterior to the heart. Furthermore, in *P. guttata guttata* ([Fig. 16A](#)) the right ductus arteriosus was becoming obliterated; in *P. curtus breitensteini*, the ductus was still apparent.

Zehr [40] stage 34–36

No specimen of *P. curtus breitensteini* was available. The lungs were in an advanced stage of development, with distinct faveoli and tracheal rings. In *Elaphe obsoleta spiloides* the left lung ([Fig. 17A](#)) featured distinct faveoli and a wide
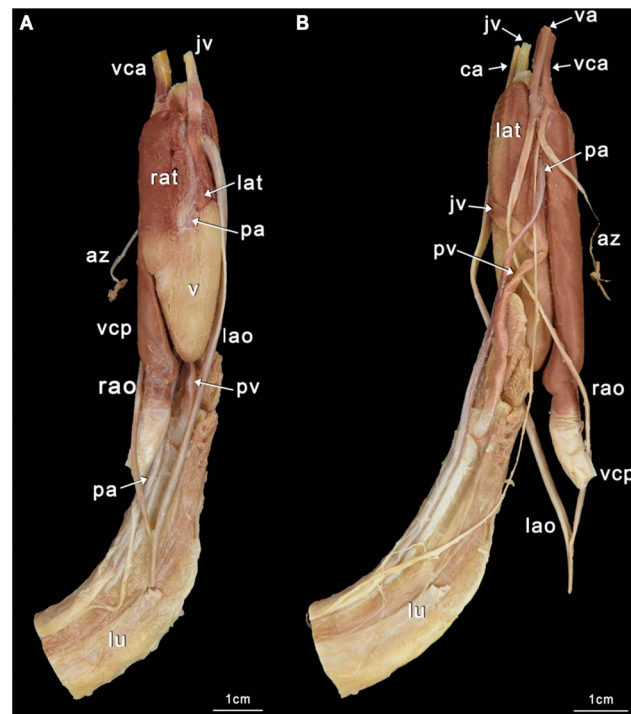
Fig. 7. The *Bungarus candidus* heart (ID BS24). A Ventral view; B Dorsal view. The lung was turned laterally by 180 degrees for the purpose of these photographs, which has detached the pulmonary vein and vena cava posterior that normally run together. az = azygous artery; ca = carotid artery; jv = jugular vein; lao = left aorta; lat = left atrium; lu = lung; pa = pulmonary artery; pv = pulmonary vein; rao = right aorta; rat = right atrium; v = ventricle; va = vertebral artery; vca = vena cava anterior; vcp = vena cava posterior.

lumen ([Fig. 10E](#)). In *Calloselasma rhodostoma* ([Fig. 17B](#)) the faveoli of the tracheal lung had reached a state of maturity apparently similar to that of the right lung. It extended until approximately halfway along the ventricle, where a gradual widening of its lumen indicated the origin of the right lung ([Fig. 12E](#)), although there was no sharp boundary between the two.

The vascular anatomy of *E. obsoleta spiloides* ([Fig. 17A](#)) and *Calloselasma rhodostoma* ([Fig. 17B](#)) were highly similar. The right ductus arteriosus was completely obliterated, although in *E. obsoleta spiloides* remnants of the right 4th and 6th PAA could still be distinguished. On the left, the ductus arteriosus persisted. Differences were found in the pulmonary artery: in *Calloselasma rhodostoma* it curved anteriorly, not posteriorly as it does in *E. obsoleta spiloides*. Additionally, at the curvature where the single pulmonary artery curves anteriorly, a second pulmonary artery branched off in a posterior direction in *Calloselasma rhodostoma*.
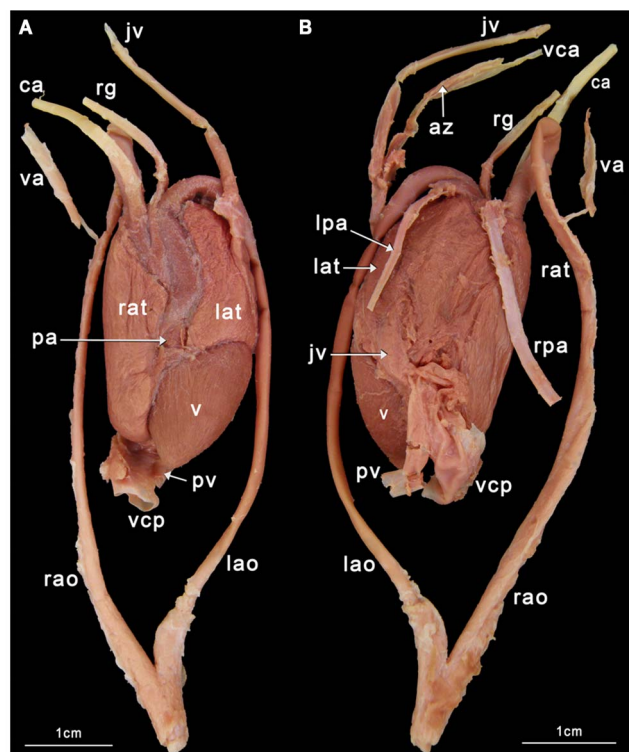
Fig. 8. The *Eunectus notaeus* heart (ID BS8). A ventral view; B dorsal view. az = azygos vein; ca = carotid artery; jv = jugular vein; lao = left aorta; lat = left atrium; pv = pulmonary vein; lpa = left pulmonary artery; rao = right aorta; rat = right atrium; rpa = right pulmonary artery; rg = ramus glandularis; v = ventricle; va = vertebral artery; vca = vena cava anterior; vcp = vena cava posterior.

doi:10.1371/journal.pone.0116416.g008

Discussion

Classification of the pulmonary arteries in the adult snake

We have examined the adult anatomy of the pulmonary arteries in a broad phylogenetic sample of snake species. We find that the adult anatomical pattern of the pulmonary arteries in the species sampled can be described under three types,

- 🟩 Right aorta/Carotid arteries
- 🟨 Left aorta
- 🟥 Dorsal aorta
- 🟦 PAA VI/Pulmonary artery
- 🟩 Right lung
- 🟨 Left lung
- 🟦 Trachea
- ⬛ Tracheal lung
- 🟪 Ductus arteriosus
- 🟧 PAAs (2dao *Pantherophis*)
- ⬜ Gut (2dao *Pantherophis*)

Fig. 9. Legend for 3D segmentations in Amira.

doi:10.1371/journal.pone.0116416.g009
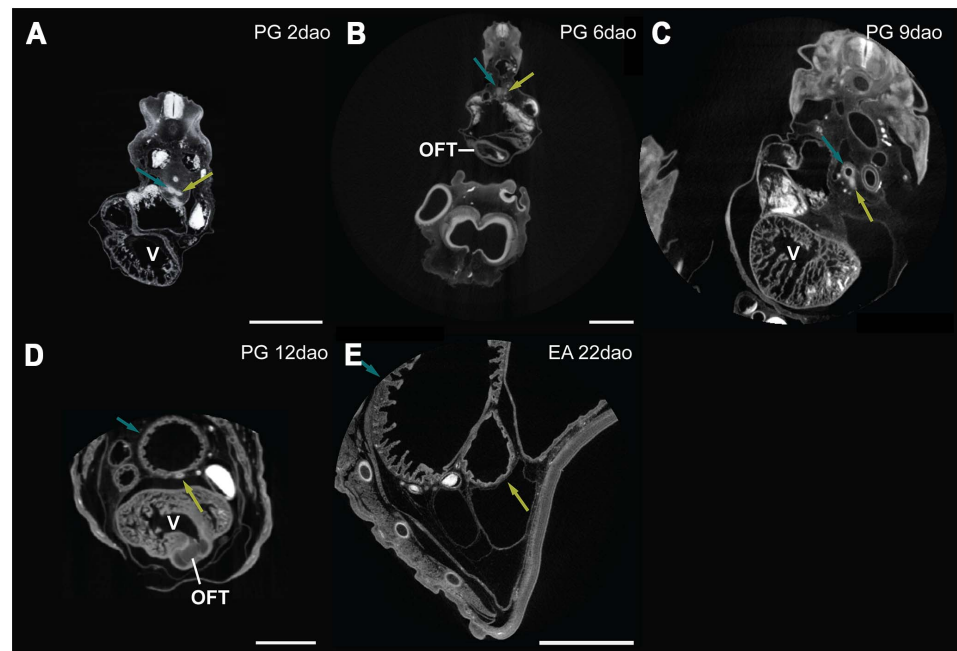
Fig. 10. MicroCT transverse sections of embryos showing lung lumina. Sections are of *Pantherophis guttata guttata* (A – D) and *Elaphe obsoleta spiloides* (E). The embryo's dorsal sides are up. Astral blue arrows denote right lung, dark yellow left lung; V = ventricle; OFT = outflow tract. Annotation done in Amira 5.4.5. Scale bar represents 1 mm.

doi:10.1371/journal.pone.0116416.g010

which we designate PA1-3. When examining published typifications [54–56], a common plan is revealed that corresponds to our type PA1. For example, Brongersma's types one and four [54] differ on a gross level only on the dorso-ventral position of the vessels. The other three Brongersma types can also be characterized as type PA1. This could be a consequence of the restricted species sample that Brongersma investigated: they are all Viperidae.

When we map our findings onto a phylogeny (Fig. 2), at least two shared primitive features in the macrostomata are recognized: the presence of an anteriorly extending pulmonary trunk and a right pulmonary artery, which can extend posteriorly or anteriorly. Of note is that *Hydrophis elegans* is the only snake with a PA type that is different from other Elapidae examined in this study. One possibility is that this is due to the lifestyle of this snake: *Hydrophis elegans* is the only purely aquatic snake [14] within the Elapidae examined by us; the others species are either terrestrial (*Bungarus candidus*, *Bungarus fasciatus*, *Lampropeltis triangulum sinaloea*, *Pantherophis guttata guttata* and *Elaphe obsoleta spiloides*) or semi-aquatic (*Natrix tesselata* and *Thamnophis sirtalis concinnus*).

Some species described in the literature but not sampled here are not easily reconciled with any one of our three types. These include *Agkistrodon contortrix mokasen* [57], *Charina bottae* [10], *Crotalus atrox* [56], *Crotalus horridus* [56], *Crotalus viridis* [56], *Elaphe obsoleta quadrivittata* [10], *Python regius* [58, 59] Family Pareatidae [60], *Sistrurus ravus* [56], and Family Typhlopidae [61]. It is
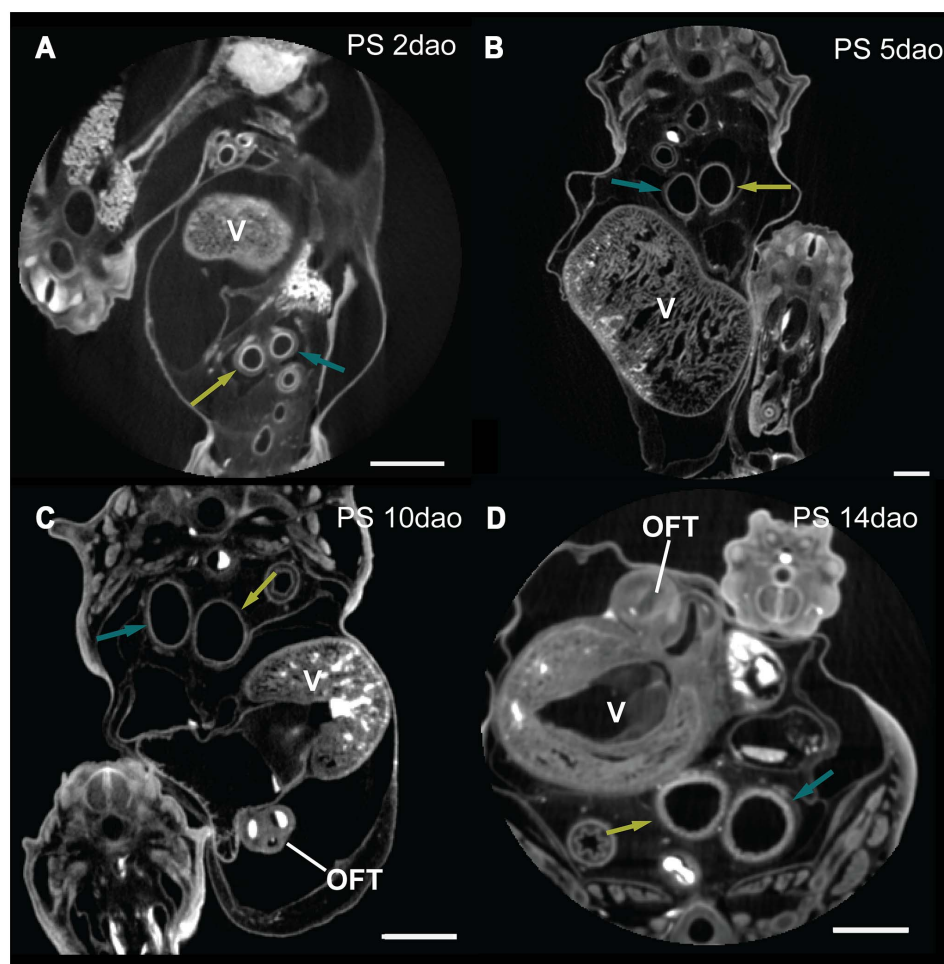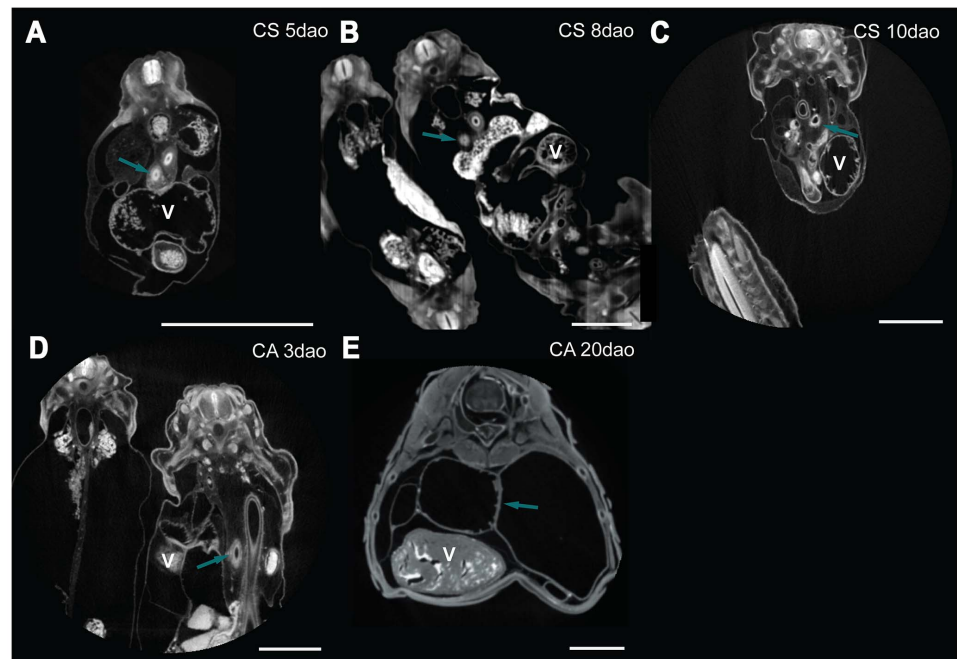
Fig. 11. MicroCT transverse sections of embryos showing lung lumina. Sections are of *Python curtus breitensteini*. The embryo's dorsal sides are up. Astral blue arrows denote right lung, dark yellow left lung; V = ventricle; OFT = outflow tract. Annotation done in Amira 5.4.5. Scale bar represents 1 mm.

not clear whether this is due to differences in interpretation, or to our limited sample size. Alternative nomenclatures, such as that used by Robb [61] for the Typhlopidae, will lead to different interpretations even if the pulmonary artery anatomy is the same.

Development of lungs and pulmonary arteries

We show that the development of lungs and the surroundings splanchnic plexus [25, 30, 31, 33, 62], which differentiate into the pulmonary arteries, is a tightly integrated process, in which some deviations from a common plan appear early. Therefore, if the left lung bud fails to develop the splanchnic plexus will not develop either. As a result, the left pulmonary artery will also not develop.

Fig. 12. MicroCT transverse sections of embryos showing lung lumina. Sections are of *Causus rhombeatus* (A – C) and *Calloselasma rhodostoma* (D, E). The embryo's dorsal sides are up. Astral blue arrows denote right lung, dark yellow left lung; V = ventricle. Annotation done in Amira 5.4.5. Scale bar represents 1 mm.

doi:10.1371/journal.pone.0116416.g012
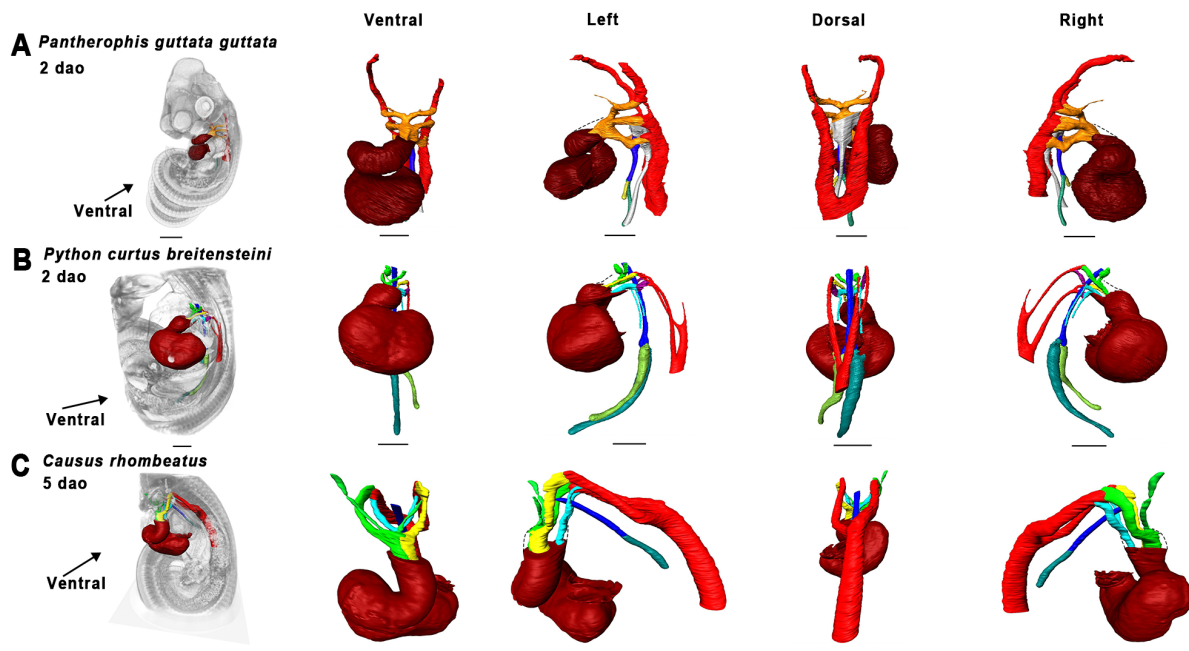
Fig. 13. Overview of 3D reconstructions comparing similar developmental stages (Zehr 22–24 [40]). Visualized species are *Pantherophis guttata guttata* (A), *Python curtus breitensteini* (B) and *Causus rhombeatus* (C). Reconstructions were made in Amira 5.4.5. Dashed lines denote outflow tract contours. Scale bars represent 1 mm.
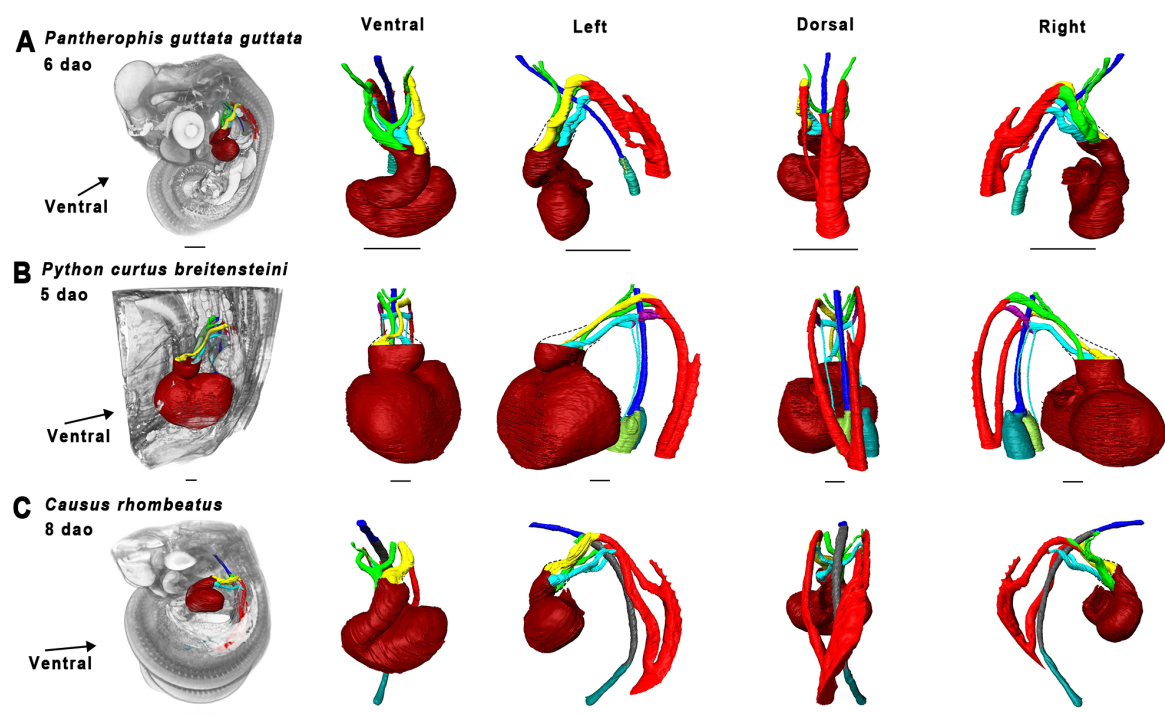
doi:10.1371/journal.pone.0116416.g013

Fig. 14. Overview of 3D reconstructions comparing similar developmental stages (Zehr 25–28 [40]). Visualized species are *Pantherophis guttata guttata* (A), *Python curtus breitensteini* (B) and *Causus rhombeatus* (C). Reconstructions were made in Amira 5.4.5. Dashed lines denote outflow tract contours. Scale bars represent 1 mm.

doi:10.1371/journal.pone.0116416.g014

Development of the right lung

The right bronchial bud is established early in development and develops into a mature right lung in all species. *Causus rhombeatus* deviates from the common plan in that it has a thoraconuchal lung in which the right lung and the tracheal lung are continuous. Already at early stages of tracheal lung development it was hard to distinguish it from the right lung. Thus, the question arises to what extent the development of right and tracheal lung are integrated. Further studies into the development of the thoraconuchal lung would therefore be of interest.

In *Calloselasma rhodostoma* the transition point from tracheal to right lung is demarcated by a constriction in the tracheal lumen at the axial level of the heart. However, this constriction disappeared at later stages of development. Regardless of the mode of development of the right lung, the right pulmonary artery always developed and became connected with the right branch of the 6th PAA. As a result, this branch always persisted to some extent, as in *Calloselasma rhodostoma*, *E. obsolete spiloides* and *P. guttata guttata* the right ductus arteriosus regressed. In *P. curtus breitensteini* we lacked developmental stages sufficiently advanced to provide more definitive conclusions.

Development of the left lung

Our data show that four developmental patterns of the left lung can be distinguished. The first (Table 5, Type 1) is characterized by absence of a left
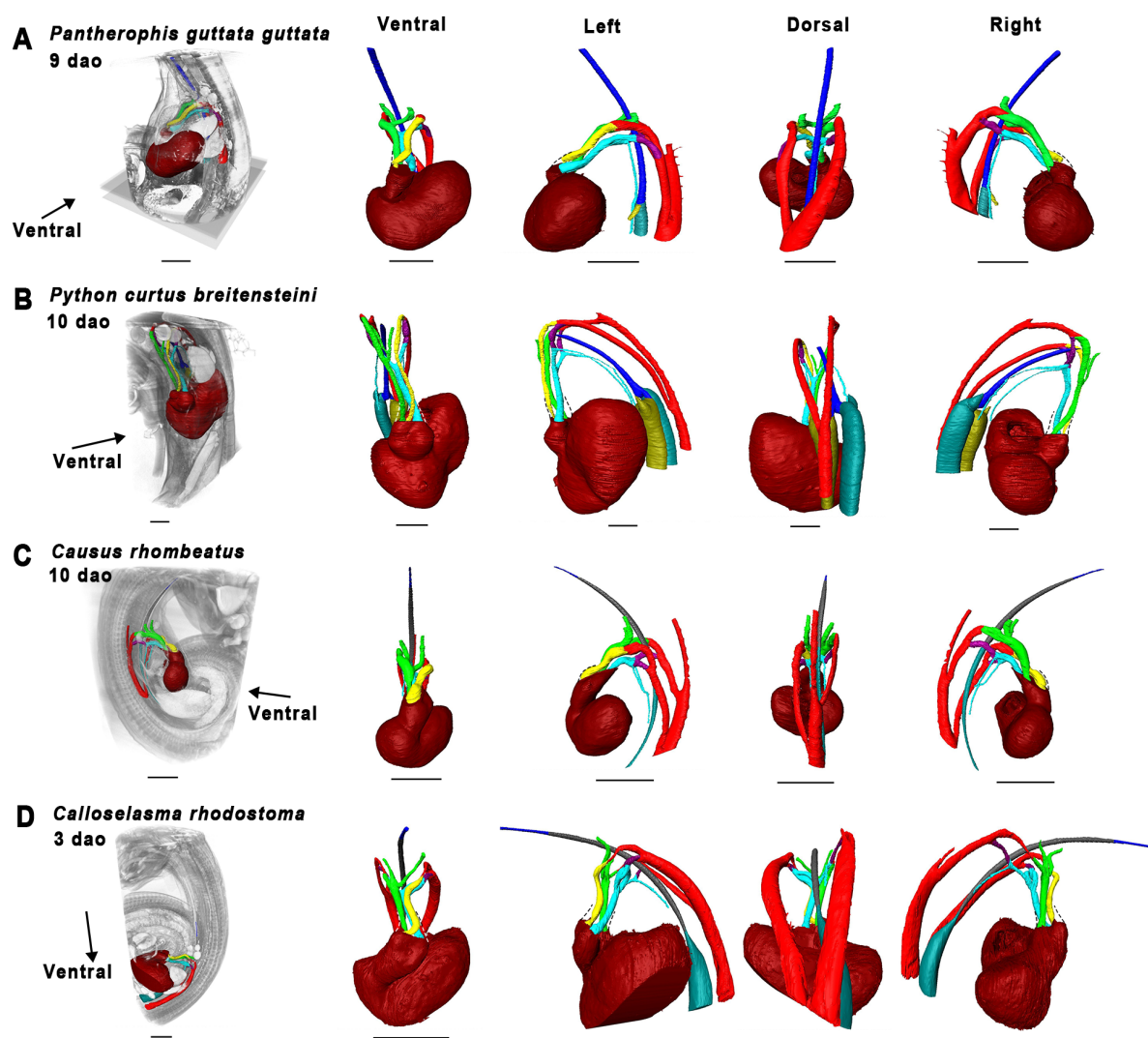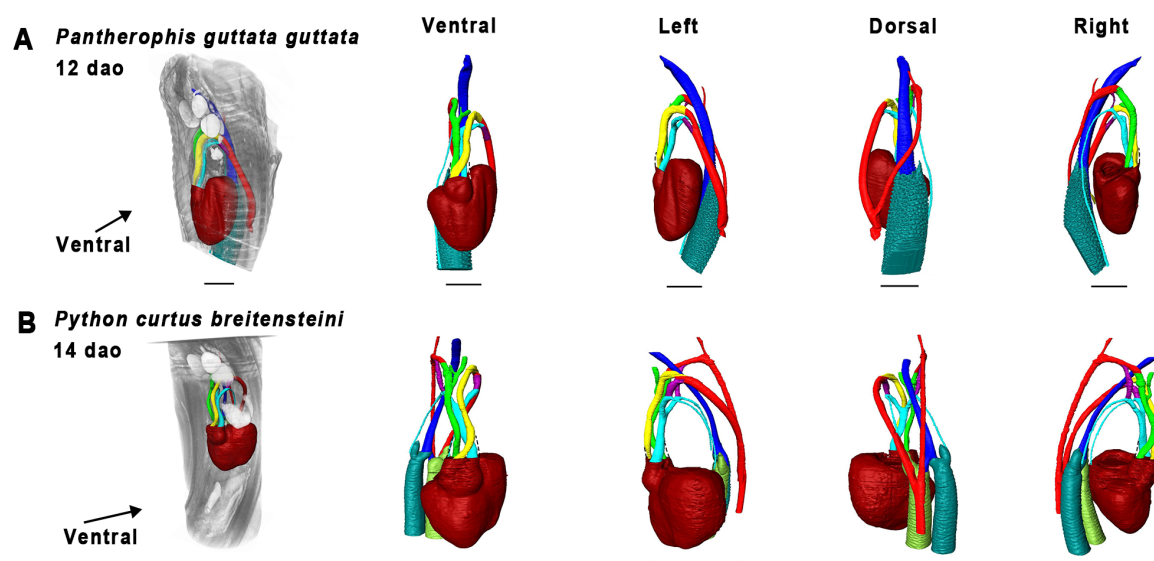
Fig. 15. Overview of 3D reconstructions comparing similar developmental stages (Zehr 26–30 [40]). Visualized species are *Pantherophis guttata guttata* (A), *Python curtus breitensteini* (B), *Causus rhombeatus* (C) and *calloselasma rhodostoma* (D). Reconstructions were made in Amira 5.4.5.Dashed lines denote outflow tract contours. Scale bars represent 1 mm.

doi:10.1371/journal.pone.0116416.g015

bronchial bud in both *Calloselasma rhodostoma* and *Causus rhombeatus*. However, we lacked the youngest of embryonic stages, so that we could not determine whether a left bronchial bud does not develop due to absence of tracheal bifurcation, or whether it regresses shortly after its formation. Both developmental patterns result in type 1 lung anatomy (Table 5).

The second and third developmental patterns (Table 5, Type 2a and 2b) were observed in snakes with a vestigial left lung. This condition implies inhibition of lung elongation, but not necessarily of lung maturation: in the majority of species the vestigial left lung is faveolated and vascularized [12], which are typical anatomical features of a mature lung. Moreover, a vascularized vestigial left lung may be served by a minute pulmonary artery [12], which indicates a contribution

Fig. 16. Overview of 3D reconstructions comparing similar developmental stages (Zehr 32–33 [40]). Visualized species are *Pantherophis guttata guttata* (A) and *Python curtus breitensteini* (B). Reconstructions were made in Amira 5.4.5. Dashed lines denote outflow tract contours. Scale bars represent 1 mm.

to respiration. We did not observe any such minute pulmonary artery in our 22 dao *E. obsolete spiloides* specimen, but it is possible that the resolution of the MicroCT scans was either insufficient to detect this artery, or its presence was
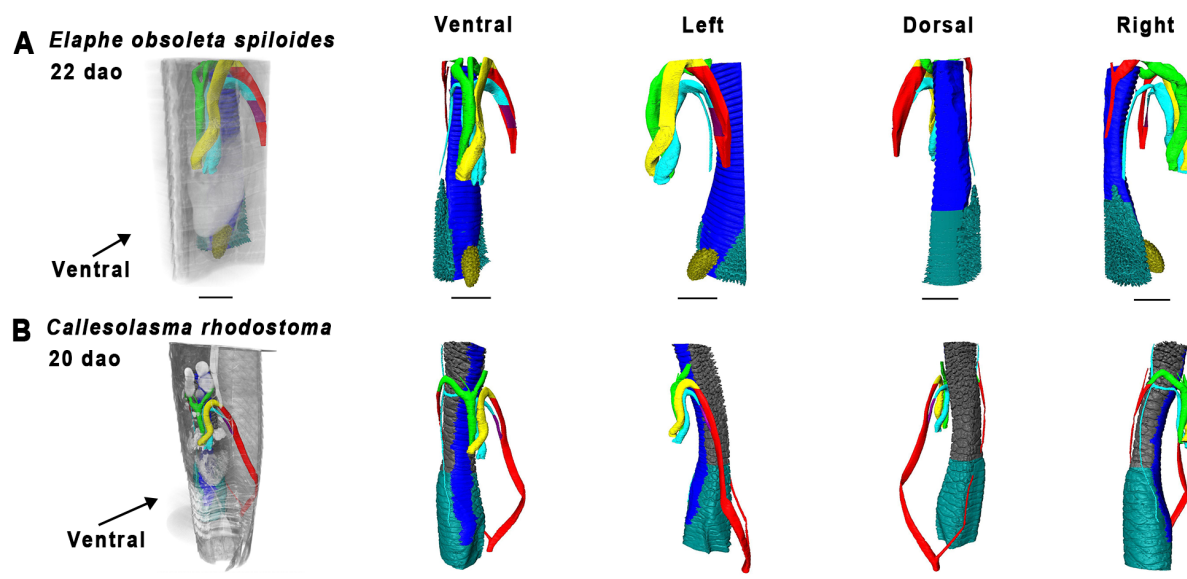
Fig. 17. Overview of 3D reconstructions comparing similar developmental stages (Zehr 34–36 [40]). Visualized species are *Elaphe obsolete spiloides* (A), and *Calloselasma rhodostoma* (B). Reconstructions were made in Amira 5.4.5. Scale bars represent 1 mm.

Table 5. Summary of some variations in the morphology of the lungs and pulmonary artery types in selected snake taxa (based on our own observations and Ref. [12]).

Development		Resulting lung pattern			Resulting PA* pattern		Taxa	
Lung development type	Description of lung development type	Left lung	Right lung	Type [12]	Left PA	Right PA	Our type	Representative taxa
1	Right lung bud develops normally; left lung bud is absent. A tracheal lung may develop from the trachea.	Absent	Fully developed	1	Absent	Present	PA1 or PA2	Acrochordidae
2a	Right lung bud develops normally; left lung bud is present but fails to elongate and no faveoli are formed. A tracheal lung may develop from the trachea.	Vestigial, not faveolated	Fully developed	2	Absent	Present	PA1 or PA2	Colubridae
2b	Right lung bud develops normally; left lung bud is present but faveoli are formed. A tracheal lung may develop from the trachea.	Vestigial, faveolated	Fully developed	2	Minute, if present	Present	PA1 or PA2	Colubridae
3	Both right and left lung buds develop normally.	Fully developed	Fully developed	3	Present	Present	PA3	Boidae

*PA = Pulmonary Artery.

doi:10.1371/journal.pone.0116416.t005

obscured by nearby structures. In the snakes that possess a vestigial left lung, it is usually both faveolated and vascularised [12].

Based on the observation that the vestigial left lung may or may not be faveolated and vascularized, the vestigial nature of the left lung may result from two processes: inhibition of early elongation of the left bronchial bud, and inhibition of later faveolization and vascularization. Thus we are able to identify two developmental patterns. In both cases the left bronchial bud undergoes significant slowing shortly after appearing, followed by arrest of elongation, and then either (1) fails to become vascularized (Table 5, Type 2a), (2) or undergoes subsequent vascularization (Table 5, Type 2b). Both development patterns result in type 2 lung anatomy (Table 5).

The fourth developmental pattern (Table 5, Type 3) leads to a fully developed, albeit relatively short left lung. The question arises whether the left lung is shorter than the right lung because it develops slower, as suggested previously [15, 63], or because its growth is arrested early (truncation). The earliest stage of *Python curtus breitensteini* in our sample (Fig. 13B) shows that the left lung is shorter than the right lung. Since already at this early stage the two lungs in this species are subequal, our data are most easily explained, in view of previous studies in *Thamnophis radix* and *Natrix natrix* [15, 24], by assuming that the left lung has a lower growth rate than the right lung, as opposed to truncation at a later stage of development. It is important to note that availability of this rare embryonic material is limited, and so it was not possible to make any quantitative determination of growth rates. It is also possible that the left lung bud initiated its development at a later stage (also a kind of heterochrony) or was smaller from the beginning (perhaps due to differences in cell allocation between the left and right buds). Further studies on a larger series of python embryos is needed to examine these issues.

To summarize, we propose that a stepwise change in developmental mechanisms resulted in the obliteration of the left lung. First, in basal macrostomata (represented by *Python curtus breitensteini* in this study), slowing of left lung elongation leads to a left lung that is shorter than the right lung. Secondly, in more advanced snakes (represented by *Pantherophis guttata guttata* and *Elaphe obsolete spiloides*), the arrest of elongation (truncation) later in left lung bud development results in a vestigial, faveolated left lung. Finally, failure to faveolate results in a vestigial left lung lacking faveoli. See Fig. 2 for a mapping of these events onto our phylogeny.

Development of the tracheal lung

Our results suggest that the tracheal lung arises as an outgrowth of respiratory tissue from the trachea. In the adult, the tracheal rings are open on the dorsal side so that the lumen of the tracheal lung and trachea communicate. Since tracheal rings are typically C-shaped [12], it is possible that respiratory tissue evaginates from the dorsal cleft in the trachea. A follow-up study investigating the specifics of tracheal lung development would be of great value. Tbx5 gene expression studies

could be of special interest, given its role in formation of the tracheal cartilage in mice [5].

We show that no distinct pulmonary artery develops in relation to the tracheal lung; instead it might be supplied by the tracheal artery, which in humans branches of the inferior thyroid artery [64]. In snakes, however, it usually branches of the carotid artery [65–70], which does not correlate with the anterior pulmonary artery described here and in the literature (S1 Table). We, therefore, suggest that the anterior pulmonary artery is either an anteriorly relocated posterior pulmonary artery (as we propose for *Calloselasma rhodostoma*), or a branch of a posterior pulmonary artery (as we propose for *Hydrophis elegans*).

The tracheal lung and associated pulmonary artery were previously proposed to be an anteriorly relocated left lung and pulmonary artery, respectively [61]. This was disproved [71] when the presence of a ligamentum arteriosum between pulmonary trunk and left aorta was highlighted in snakes lacking a left pulmonary artery, which agrees with our results; the anterior pulmonary artery can therefore not be analogous with the left pulmonary artery.

We here propose a new hypothesis: descent of the heart, cephalic folding and elongation of the neck during development cause a change in pulmonary artery location with respect to the heart. While the lungs remain in a relatively stable location, the heart will pass the location where the pulmonary arteries attach to the lung. An embryonic posterior pulmonary artery will thus become relocated to an anterior position. Our observation in 20 dao *Calloselasma rhodostoma* is thus easily explained. In this species, the pulmonary artery curved posteriorly in early stages, but anteriorly in late stages. Additionally, the posterior branch was but a branch off the anteriorly curving pulmonary artery. This resembles our dissected *Trimeresurus* heart, and the same applies to *Causus rhombeatus*, whose adults are reported to exhibit two anterior pulmonary arteries [54]: it is a flipped version of the embryonic pulmonary artery anatomy found in this study.

Some snakes however, with have respiratory tissue along the entire longitudinal axis of the body [14], will have respiratory tissue posterior to the heart even after the descent of the heart, such as *Hydrophis* (Fig. 8). In this species the primary pulmonary artery in this species is likely not the anterior one but the posterior one. Further research into the development of such secondary pulmonary arteries is warranted.

Conclusion

We have studied the development of the lungs and pulmonary arteries in snakes. We conclude that right and tracheal lung each develops via a common plan across species. By contrast, the left lung bud may (1) never develop; (2) become arrested after tracheal bifurcation, either without (2a) or with (2b) subsequent development of faveoli and vascularisation; (3) or elongate and differentiate normally, but at a slower rate than the right. The pulmonary arteries develop from locations posterior to the heart, but only if the relevant lung is functionally

significant. No pulmonary artery develops in relation to the tracheal lung. Instead we propose that descent of the heart down the body, cephalic folding and elongation of the neck cause the heart to shift to a more posterior location with respect to the lung. A right posterior pulmonary artery may thus become a right anterior pulmonary artery.

This study shows that asymmetry in the snake respiratory system manifests itself early in development. This is in accordance with an earlier study [15]. It therefore seems likely that lung asymmetry appeared in the common ancestor to the serpentes, as opposed to having evolved independently several times. This suggests that the ancestral condition was one of pulmonary symmetry, as suggested by Kardong [10]. Reconstruction of further evolutionary events leading to the current asymmetrical pattern in the snake respiratory system requires more data. We propose that the left lung was gradually obliterated due to an in series placement of several developmental mechanisms: slowed elongation, truncation and failure to faveolate. However, it is also possible that, from the ancestral condition, the right lung has elongated and the ancestral length of the left lung persisted. It is also possible that a combination of these events took place.

We recommend that future work be aimed at exploring the development of additional snake species, and elucidating the genetic mechanisms influencing the various left and right lung growth rates. These should then be compared with developmental mechanisms of the lungs in relevant outgroups (such as *Anolis* or *Pogona*). Studies in mouse suggest that regulatory genes such as Tbx4, Tbx5 and Pitx2 are involved in patterning of the lungs, and thus the manifestation of asymmetry. However, left and right lung growth speeds might be mediated independently from each other by Shh [72] and sprouty [73] (see for reviews Refs. [1, 2, 7, 74]). Using the data provided by this study on the timing of developmental events in the snake respiratory system, it has become possible to study the involvement of these genes in the development of the snake respiratory system.

Supporting Information

S1 Table. Overview of all literature dealing with cardiopulmonary connections known to us, including other observations (if available). Note that the data on the direction and number of cardiopulmonary connection vessels have been simplified; extensive detail of the original literature made it hard to summarize the data otherwise. L Type = lung type (based on [12]), nPA = number of pulmonary arteries, Direct. PA = direction of the pulmonary artery, nPV = number of pulmonary veins, Direct PV = direction of the pulmonary vein, Heart pos. = Heart position along long body axis.
doi:10.1371/journal.pone.0116416.s001 (DOC)

Acknowledgments

Author Contributions

References

1. **Metzger RJ, Klein OD, Martin GR, Krasnow MA** (2008) The branching programme of mouse lung development. Nature 453: 745–750.

2. **Cardoso WV, Lü J** (2006) Regulation of early lung morphogenesis: questions, facts and controversies. Development 133: 1611–1624.

3. **Cardoso WV** (2001) Molecular regulation of lung development. Annu Rev Physiol 63: 471–494.

4. **Lin CR, Kioussi C, O'Connell S, Briata P, Szeto D, et al.** (1999) Pitx2 regulates lung asymmetry, cardiac positioning and pituitary and tooth morphogenesis. Nature 401: 279–282.

5. **Arora R, Metzger RJ, Papaioannou VE** (2012) Multiple roles and interactions of Tbx4 and Tbx5 in development of the respiratory system. PLoS Genet 8: e1002866.

6. **Metzger RJ** (1999) Genetic Control of Branching Morphogenesis. Science (80–) 284: 1635–1639.

7. **Maina JN** (2012) Comparative molecular developmental aspects of the mammalian- and the avian lungs, and the insectan tracheal system by branching morphogenesis: recent advances and future directions. Front Zool 9: 16.

8. **Sutherland DC, Samakovlis C, Krasnow MA** (1996) branchless encodes a Drosophila FGF homolog that controls tracheal cell migration and the pattern of branching. Cell 87: 1091–1101.

9. **Klambt C, Glazer L, Shilo BZ** (1992) breathless, a Drosophila FGF receptor homolog, is essential for migration of tracheal and specific midline glial cells. Genes Dev 6: 1668–1678.

10. **Kardong K V** (1972) Morphology of the respiratory system and its musculature in different snake genera. Gegenbaurs Morphol Jahrbuch, Leipzig 117: 285–302.

11. **Perry SF** (1998) Lungs: comparative anatomy, functional morphology, and evolution. In: Gans C, Gaunt AS, editors. Biology of the Reptilia Vol.19 (Morphology G). Ithaka, New York, Vol. 19. pp. 1–92.

12. **Wallach V** (1998) The Lungs of Snakes. In: Gans C, Gaunt AS, editors. Biology of the Reptilia Vol.19 (Morphology G). Ithaka, New York: SSAR Press. pp. 93–283.

13. **Wang T, Smits AW, Burggren WW** (1998) Pulmonary function in reptiles. In: Gans C, Gaunt AS, editors. Biology of the Reptilia Vol.19 (Morphology G). Ithaka, New York: SSAR Press. pp. 297–373.

14. **Lillywhite HB, Albert JS, Sheehy CM, Seymour RS** (2012) Gravity and the evolution of cardiopulmonary morphology in snakes. Comp Biochem Physiol A Mol Integr Physiol 161: 230–242.

15. **Schmalhausen JJ** (1905) Die entwickelung der Lungen bei Tropidonotus natrix. Anat Anz: 511–520.

16. **Ten Have-Opbroek AAW** (1991) Lung development in the mouse embryo. Exp Lung Res 17: 111–130.

17. **Sadler TW** (2012) Respiratory System. Langman's Medical Embryology. p. 384.

18. **Gould SJ** (1977) Ontogeny and Phylogeny. Cambridge, Massachusetts: Belknap Press of Harvard University Press.

19. **Klingenberg CP** (1998) Heterochrony and allometry: the analysis of evolutionary change in ontogeny. Biol Rev Camb Philos Soc 73: 79–123.

20. **Smith KK** (2003) Time's arrow: heterochrony and the evolution of development. Int J Dev Biol 621: 613–621.

21. **De Jong IML, Colbert MW, Witte F, Richardson MK** (2009) Polymorphism in developmental timing: intraspecific heterochrony in a Lake Victoria cichlid. Evol Dev 11: 625–635.

22. **Mabee PM, Olmstead KL, Cubbage CC** (2000) An experimental study of intraspecific variation, developmental timing, and heterochrony in fishes. Evolution 54: 2091–2106.

23. **Richardson MK** (1995) Heterochony and the phylotypic period. Dev Biol 172: 412–421.

24. **Harrison BM, Denning NE** (1929) Embryonic development of the pharyngeal region in Thamnophis radix. Anat Rec 44: 101–116.

25. **DeRuiter MC, Gittenberger-de Groot AC, Poelmann RE, VanIperen L, Mentink MM** (1993) Development of the pharyngeal arch system related to the pulmonary and bronchial vessels in the avian embryo. With a concept on systemic- pulmonary collateral artery formation. Circulation 87: 1306–1319.

26. **DeMello DE, Sawyer D, Galvin N, Reid LM** (1997) Early fetal development of lung vasculature. Am J Respir Cell Mol Biol 16: 568–581.

27. **Hall SM, Hislop AA, Pierce CM, Haworth SG** (2000) Prenatal origins of human intrapulmonary arteries: formation and smooth muscle maturation. Am J Respir Cell Mol Biol 23: 194–203.

28. **Hislop AA, Pierce CM** (2000) Growth of the vascular tree. Paediatr Respir Rev 1: 321–327.

29. **Hislop AA** (2002) Airway and blood vessel interaction during lung development. J Anat 201: 325–334.

30. **Hislop AA** (2005) Developmental biology of the pulmonary circulation. Paediatr Respir Rev 6: 35–43.

31. **Anderson-Berry A, O'Brien EA, Bleyl SB, Lawson A, Gundersen N, et al.** (2005) Vasculogenesis drives pulmonary vascular growth in the developing chick embryo. Dev Dyn 233: 145–153.

32. **Fisher KA, Summer RS** (2006) Stem and progenitor cells in the formation of the pulmonary vasculature. Curr Top Dev Biol 74: 117–131.

33. **Schachtner SK, Wang Y, Scott Baldwin H** (2000) Qualitative and quantitative analysis of embryonic pulmonary vessel formation. Am J Respir Cell Mol Biol 22: 157–165.

34. **Langer A** (1894) Über die Entwicklungsgeschichte des Bulbus Cordis bei Amphibien und Reptilien. Morphol Jahrb 21: 40–68.

35. **Greil A** (1903) Beiträge zur vergleichenden Anatomie und Entwicklungsgeschichte des Herzens und des Truncus Arteriosus der Wirbelthiere. Morphol Jahrb 31: 123–310.

36. **Goodrich ES** (1958) Studies on the structure and development of vertebrates. New York: Dover Publications.

37. **Shaner RF** (1962) Comparative Development of the Bulbus and Ventricles if the vertebrate Heart with Species Reference to Spitzer's Theory of Heart malformations. Anat Rec 142: 519–529.

38. **Hart NH** (1968) Formation of Septa in the Bulbus Cordis of a Turtle and a Lizard. J Morphol 125: 1–22.

39. **Hart NH** (1969) The bulbus cordis and its septa in Sphenodon punctatus. J Morphol 129: 369–374.

40. **Zehr DR** (1962) Stages in the normal development of the common Garter Snake, Thamnophis sirtalis sirtalis. Copeia 2: 322–329.

41. **Jackson K** (2002) Post-ovipositional development of the monocled cobra, Naja kaouthia (Serpentes: Elapidae). Zoology 105: 203–214.

42. **Khannoon ER, Evans SE** (2014) The embryonic development of the Egyptian cobra Naja h. haje (Squamata: Serpentes: Elapidae). Acta Zool 95: 472–483.

43. **Boback SM, Dichter EK, Mistry HL** (2012) A developmental staging series for the African house snake, Boaedon (Lamprophis) fuliginosus. Zoology 115: 38–46.

44. **Boughner JC, Buchtová M, Fu K, Diewert V, Hallgrímsson B, et al.** (2007) Embryonic development of Python sebae - I: Staging criteria and macroscopic skeletal morphogenesis of the head and limbs. Zoology 110: 212–230.

45. **Buchtová M, Boughner JC, Fu K, Diewert VM, Richman JM** (2007) Embryonic development of Python sebae - II: Craniofacial microscopic anatomy, cell proliferation and apoptosis. Zoology 110: 231–251.

46. **Vidal N** (2002) Colubroid Systematics: Evidence for an Early Appearance of the Venom Apparatus Followed By Extensive Evolutionary Tinkering. Toxin Rev 21: 21–41.

47. **Vidal N, Hedges SB** (2002) Higher-level relationships of snakes inferred from four nuclear and mitochondrial genes. C R Biol 325: 977–985.

48. **Vidal N, Delmas A-S, David P, Cruaud C, Couloux A, et al.** (2007) The phylogeny and classification of caenophidian snakes inferred from seven nuclear protein-coding genes. C R Biol 330: 182–187.

49. **Pyron RA, Burbrink FT, Colli GR, de Oca ANM, Vitt LJ, et al.** (2011) The phylogeny of advanced snakes (Colubroidea), with discovery of a new subfamily and comparison of support methods for likelihood trees. Mol Phylogenet Evol 58: 329–342.

50. **Zaher H, Grazziotin FG, Cadle JE, Murphy RW, De Moura-Leite JC, et al.** (2009) Molecular phylogeny of advanced snakes (Serpentes, Caenophidia) with an emphasis on South American Xenodontines: a revised classification and descriptions of new taxa. Papéis Avulsos Zool 49: 115–153.

51. **Metscher BD** (2009) MicroCT for developmental biology: a versatile tool for high-contrast 3D imaging at histological resolutions. Dev Dyn 238: 632–640.

52. **Schulz-Mirbach T, Heß M, Metscher BD** (2013) Sensory epithelia of the fish inner ear in 3D: studied with high-resolution contrast enhanced microCT. Front Zool 10: 63.

53. **Metscher BD** (2011) X-ray microtomographic imaging of intact vertebrate embryos. Cold Spring Harb Protoc 2011: 1462–1471.

54. **Brongersma LD** (1949) On the main branches of the pulmonary artery in some viperidae. Bijdr tot Dierkd 28: 57–64.

55. **Brongersma LD** (1951) Some remarks on the pulmonary artery in snakes with two lungs. Zool Verh 14: 3–36.

56. **Van Bourgondien TM, Bothner RC** (1969) A Comparative Study of the Arterial Systems of Some New World Crotalinae (Reptilia: Ophidia). Am Midl Nat 81: 107–147.

57. **Bothner RC** (1959) The gross anatomy of the heart and neighboring vessels in the northern subspecies of the copperhead, Agkistrodon contortrix mokeson (Daudin). Sci Stud (St Bonaventure) 20.

58. **Jensen B, Nyengaard J, Pedersen M, Wang T** (2010) Anatomy of the python heart. Anat Sci Int 85: 194–203.

59. **Starck JM** (2009) Functional Morphology and Patterns of Blood Flow in the Heart of Python regius. J Morphol 687: 673–687.

60. **Brongersma LD** (1957) Notes upon the trachea, lungs, and the pulmonary artery in snakes III. Proc K Ned Akad van Wet Ser C 60: 451–457.

61. **Robb J** (1960) The internal anatomy of Typhlops Schneider (Reptilia). Aust J Zool 8: 181–216.

62. **Molin DGM, DeRuiter MC, Wisse LJ, Azhar M, Doetschman T, et al.** (2002) Altered apoptosis pattern during pharyngeal arch artery remodelling is associated with aortic arch malformations in Tgfbeta2 knock-out mice. Cardiovasc Res 56: 312–322.

63. **Mehnert E** (1898) Biomechanik erschlossen aus dem principe der organogenese. Jena: Gustav Fischer.

64. **Salassa JR, Pearson BW, Payne WS** (1977) Gross and Microscopical Blood Supply of the Trachea. Ann Thorac Surg 24: 100–107.

65. **Atwood WH** (1916) The visceral anatomy of the blacksnake (Zamenis constrictor). Washingt Univ Stud 4: 3–38.

66. **Atwood WH** (1918) The visceral anatomy of the Garter snake. Trans Wisconsin Acad Sci Arts Lett 19: 531–552.

67. **O'Donoghue CH** (1912) The circulatory system of the common grass snake. Proceedings of the Zoological Society of London. pp. 612–647.

68. **Kashyap H V, Sohoni PR** (1973) The heart and arterial system of Acrochordus granulatus. J Univ Bombay 42: 34–52.

69. **Ray HC** (1934) On the arterial system of the common Indian rat-snake, Ptyas Mucosus (Linn.). J Morphol 56: 533–575.

70. **De Silva PHDH** (1953) The arterial system in Ceylon snakes – naja naja naja. Spolia Zeylan 27: 47–58.

71. **Brongersma LD** (1960) Tracheale of linker long? Versl van gewone Vergad van Afd Natuurkd van K Ned Akad van Wet 69: 125–128.

72. **Bellusci S, Furuta Y, Rush MG, Henderson R, Winnier G, et al.** (1997) Involvement of Sonic hedgehog (Shh) in mouse embryonic lung growth and morphogenesis. Development 124: 53–63.

73. **Hacohen N, Kramer S, Sutherland DC, Hiromi Y, Krasnow MA** (1998) sprouty Encodes a Novel Antagonist of FGF Signaling that Patterns Apical Branching of the Drosophila Airways. Cell 92: 253–263.

74. **Rawlins EL** (2011) The building blocks of mammalian lung development. Dev Dyn 240: 463–476.

75. **McDonald HS** (1959) Respiratory Functions of the Ophidian Air Sac. Herpetologica 15: 193–198.

76. **Brongersma LD** (1951) On the arteria pulmonalis in the Boidae and in some other snakes. Arch Néerlandaises Zool 10: 514.

77. **Brongersma LD** (1951) Some notes upon the anatomy of Tropidophis and Trachyboa (Serpentes). Zool Meded 31: 107–124.

78. **Brongersma LD** (1951) De arteria pulmonalis bij Boidae en bij Xenopeltis (Serpentes). Ned Tijdschr voor Geneeskd 95: 2490–2491.

79. **Brongersma LD** (1952) On the tracheal lung and lung in Acrochordus and some other snakes. Arch Néerlandaises Zool 9: 561–562.

80. **Brongersma LD** (1952) Notes upon the arteries of the lungs in Python reticulatus (Schn.). Proc K Ned Akad van Wet Ser C 55: 62–73.

81. **Brongersma LD** (1957) Notes upon the trachea, lungs, and the pulmonary artery in snakes I. Proc K Ned Akad van Wet Ser C 60: 299–308.

82. **Brongersma LD** (1957) Notes upon the trachea, lungs, and the pulmonary artery in snakes II. Proc K Ned Akad van Wet Ser C 60: 309–313.